

## MARS PATHFINDER: PHOTOGRAMMETRIC PROCESSING OF LANDER IMAGES

J. Oberst, E. Hauber, F. Trauthan, M. Kuschel, B. Giese, T. Roatsch, R. Jaumann  
DLR Institute of Planetary Exploration, Berlin, Germany  
Fax: +49/30/67055-402; E-mail: Juergen.Oberst@dlr.de

### ABSTRACT

The Mars Pathfinder stereo camera (IMP) produced a set of images unique in what they show and unique in the methods they require for their analysis and processing: We first studied the ability of the camera to carry out distance and object size measurements. Pointing of the images was calibrated using sunrise and sunset images to obtain a reference horizon mosaic having precise orientation with respect to North. Images were then processed to derive a full monoscopic color panorama, a DTM, a slope map, and various thematic maps, showing light incidence and emission angles near the landing site. These data products will greatly help geologists in their studies of the landing site.

### 1 INTRODUCTION

The primary goal of the Mars Pathfinder project was the development of a simple, low cost system that could place a science payload on the Martian surface (Golombek, 1997). The spacecraft landed successfully on July 4, 1997, and was operating through September 27, 1997, when the last data transmission cycle was completed. The mission returned 2.6 Gigabits of data, among them over 16,000 images obtained by the lander camera and 550 images from the rover cameras. These unique pictures show a slightly undulating plain which is scattered with pebbles, cobbles, and boulders. Streamlined islands, large knobs, and crater rims are visible at the horizon (Golombek *et al.*, 1997b). Owing to the diversity of the site, the image data pose a great challenge for cartographic and photogeological mapping of the area.

A large number of institutions and individuals were involved in the analysis of data from Pathfinder. While DLR's work contributions to the Pathfinder science team included geo-morphologic and photometric studies, this paper reports on the photogrammetric techniques that were used to map the lander area and on the data products that were generated to support geologists in their analysis of the terrain.

### 2 LANDER, CAMERA, AND IMAGES

The lander was equipped with a small set of instruments for a variety of science experiments (Fig. 1). This included sensors for atmospheric pressure and temperature measurements ("ASI/MET" instrument; Seiff *et al.*, 1997) and detectors for wind direction and speed. A small rover, "Sojourner", was deployed off a ramp to study the chemistry of rocks in the neighborhood of the landing site (Rover Team, 1997; Rieder *et al.*, 1997).

The principle science instrument on the lander was the IMP (Imager for Mars Pathfinder; Smith *et al.*, 1997a), a binocular CCD-based stereo camera featuring twin lenses, mounted 15 cm apart (Fig. 2). The two optical axes had a toe-in of 5.9° (37.1 rad) for optimum stereo imaging in a range from the lander between 2-10 m. The optical paths from the two lenses were combined on a 512 x 512 CCD which was divided into three major areas (Fig. 3); one stereo exposure resulted in two images, 248 x 256 pixels each with horizontal and vertical fields of view of 14.4° x 14.0°, respectively. The filter wheels, having 12 filter positions each, were mounted within the two optical paths

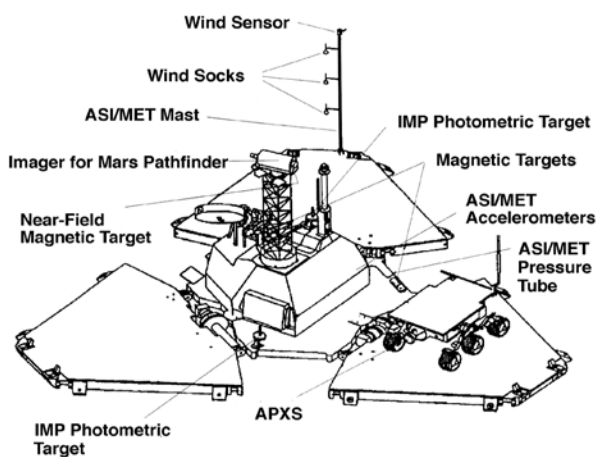


Fig. 1: Pathfinder and the rover *Sojourner*.

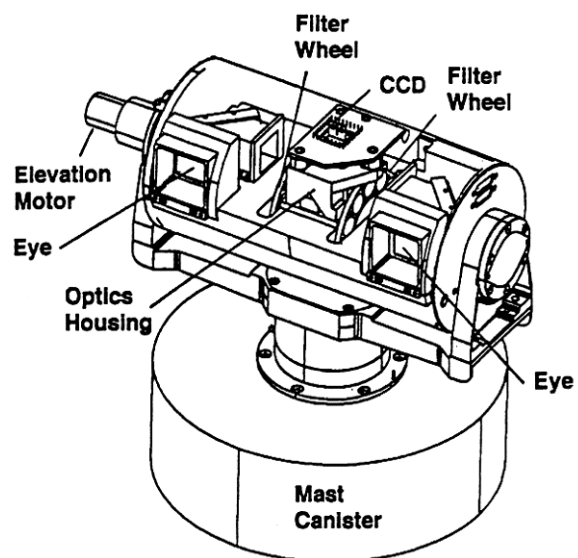


Fig. 2: Schematic view of the *Imager for Pathfinder*.

for color imaging in the wavelength range of 400-1,100 nm. The camera was installed on a boom, which raised the instrument to a height of 79 cm above the lander base (approx. 1.40 m above the ground). The camera was permitted to rotate about 360° in the horizontal plane and through elevation angles of 170°, thus making it possible to take images of the sky. Several types of data compression, lossless compression, modified JPEG compression, subframing, row-and column averaging, were used to reduce the volume of data before transmission to Earth.

During both the nominal and extended mission, the IMP camera returned 16,661 images (Smith *et al.* 1997b). Owing to the small image sizes, it became a primary photogrammetric task to produce image or DTM mosaics for the complete and contiguous coverage of the landing site. In order to obtain a complete monoscopic 360° image panorama with a single filter, approx. 150 images were required (assuming 10% image overlap). A total of five panoramic datasets with more than 3,500 images were acquired (Table 1).

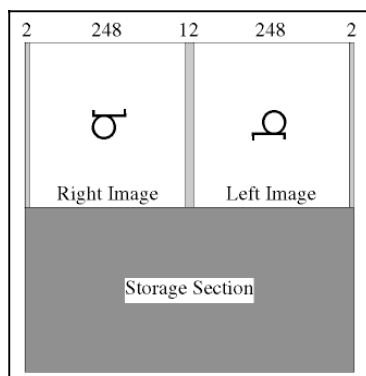


Fig. 3: Schematic view of the CCD system of the IMP camera. The two 248x256 pixel sub-arrays (one for each eye) are separated by a 12 pixel dead zone to minimize cross-talk. Electronic shutter is provided by a 512x256 readout zone. A two pixel wide border is on each edge of the CCD (Figure modified from Britt *et al.*, 1997). Note how the letter "b" is depicted on each "eye" of the

edge of the CCD (Figure modified from Britt *et al.*, 1997). Note how the letter "b" is depicted on each "eye" of the



Fig. 4: Pathfinder stereo images in the view of the IP tool, designed for manual collection of tiepoints. CCD chip due to the various mirrors in the two optical paths.

Camera Position	Lossy Data Compression	Lossless Data Compression
un-deployed	<u>First Look Panorama</u> <ul style="list-style-type: none"> <li>right eye R (filter 5)</li> <li>1/2 by azimuth</li> <li>right eye RGB (filters 5,9,0)</li> <li>&lt; 1/2 by azimuth</li> <li>red stereo</li> </ul>	<u>Insurance Panorama</u> <ul style="list-style-type: none"> <li>stereo B (filter 0)</li> <li>right eye filters 6,8,9</li> </ul>
deployed	<u>Monster Panorama</u> <ul style="list-style-type: none"> <li>red stereo</li> <li>1/2 by elevation</li> <li>right eye RGB</li> <li>quadrants at 4 times of day</li> <li><u>Gallery Panorama</u></li> <li>right eye RGB</li> <li>continuous time of day</li> </ul>	<u>Super Panorama</u> <ul style="list-style-type: none"> <li>RGB stereo</li> <li>all other filters 2:1 (near lossless)</li> <li>"patchwork" of times of day</li> <li>complete to 90%</li> </ul>

Table 1: Pathfinder cartographic imaging sequences (R: red. G: green. B: blue; modified after Gaddis *et al.*, 1998).

### 3 SOFTWARE

The photogrammetric techniques we applied to the IMP data were realized in a number of software packages that either were supplied by Pathfinder support personnel at JPL (Jet Propulsion Laboratory, Pasadena), and others that the authors from DLR specifically developed for the mission. JPL- and DLR image matchers were used to extract conjugate points from image pairs. JPL-supplied software was used to carry out one of the most crucial software tasks, to convert matched points to object points, taking into account camera constants, as determined in the calibration laboratory. JPL software and DLR-modified versions thereof were used to interpolate between object points and to produce DTM- and image mosaics and panoramas. Block adjustment software and a number of interactive tools were written from scratch. The latter were used to make tiepoint (Fig. 4), point distance, or slope measurements, to extract elevation profiles from the DTM, and to generate catalogs of rocks.

### 4 COORDINATE SYSTEMS

The Mars Pathfinder Lander coordinate definition (L) frame is right handed, orthogonal and defined by the axes  $X_L$ ,  $Y_L$ , and  $Z_L$ , where X and Y are in the plane of the lander petal, with Y pointed to the rover petal (Fig. 1) and Z pointed downward (Mellstrom and Lau, 1996). Coordinates of a number of fiducial marks on the lander base had been measured in the laboratory (Table 2) and defined this coordinate system.

Fiducial Mark	$X_L$	$Y_L$	$Z_L$
IMP Mast Origin	-0.1984	-0.009	-0.4367
IMP Stowed Origin	-0.1984	-0.009	-0.6119
IMP Deployed Origin	-0.1984	-0.009	-1.2304
Rover Ramp +X Side	0.6272	0.9750	0.0000
Rover Ramp -X Side	-0.6294	0.9751	0.0063
ASI/MET	1.4404	-0.8420	-0.6534
Middle Windsock			

Table 2: Selected coordinates of fiducial marks in the L-

frame in m

The Mars Local Level Coordinate (M) frame is right handed, orthogonal, and defined by the axes  $X_M$ ,  $Y_M$ , and  $Z_M$ , pointed North, East, and downward, respectively. The origin is coincident with the lander L frame. There are no translations in any directions with respect to the L frame, in spite of the fact that the lander base is located above the ground. Coordinates in the M frame can easily be related to the Mars body fixed frame using the known radius, areocentric latitude, and longitude of the lander (see companion paper, Oberst *et al.*, 1998). In some cartographic products, derived during the mission (Kirk *et al.*, 1998), this M coordinate system was modified so the Z direction would point upward.

Initially, the relationship between the coordinate systems was determined automatically by onboard tiltmeters and by measurements of the North direction using the camera. IMP was programmed to take images of the sky and to carry out a Sun search on the first day of the mission. These data were processed on board to determine the North direction and the position of Earth in the sky (which was needed to point the high-gain antenna). This procedure resulted in a crude estimate of the North direction, accurate to within IMP's pointing uncertainty of  $1^\circ$  (Kirk *et al.*, 1998). North direction and tilt were usually expressed in the form of a quaternion to fully describe the relationship between the two coordinate systems. The lander was determined to be tilted by  $3.9^\circ$ , with its Y axis (the petal on which the rover was located) pointed slightly upward and in the direction of  $156^\circ$  azimuth (approx. East).

Unfortunately, there were no images that allowed us to relate the positions of fiducial marks on the lander to the surrounding terrain. Thus, the relationship between the M- or the L-coordinate systems and the terrain as seen in the images initially remained uncertain to within the camera's pointing errors.

## 5 ANALYSIS OF CAMERA PERFORMANCE

Toe-in and boresight error angles of the IMP camera "stereo" filters had been carefully calibrated in the laboratory (Britt *et al.*, 1997). There was a concern that these angles might have changed during flight. Another concern was that some of the photogrammetric algorithms used in the software supplied by JPL were not transparent. In particular, the geometric parameters of the camera, used to convert conjugate image points to object coordinates, were hardcoded in the software. We therefore deemed it necessary to verify the geometric properties of the camera and the performance of the software, with the goal to analyze our ability to carry out precise distance and size measurements of objects.

### *Theoretical Errors in Distance Measurements*

We computed the theoretical errors in distance measurements from stereo images by analysis of conditions for viewing rays to intersect based on the nominal parameters of the camera optical system. We find that errors in distance measurements using stereo pairs increase with the square of distance from the lander (Fig. 5), owing to reported systematic errors in the toe-in angles of  $0.5$  mrad and the limited accuracy of conjugate point coordinate measurements. Errors in the pixel coordinates

were estimated to be  $0.2$  pixels ( $=0.196$  mrad) on average. We observed that the matching accuracy was better at near range than at far range, presumably, because of the higher contrast of features in the foreground. The distance error owing to each of these effects is approx. 3% and 10%, respectively, at a range of 30m (see Fig. 5). In practice, range measurements were found to become unacceptably large at distances beyond 50 m, as became obvious by inspection of miss distances of the viewing rays.

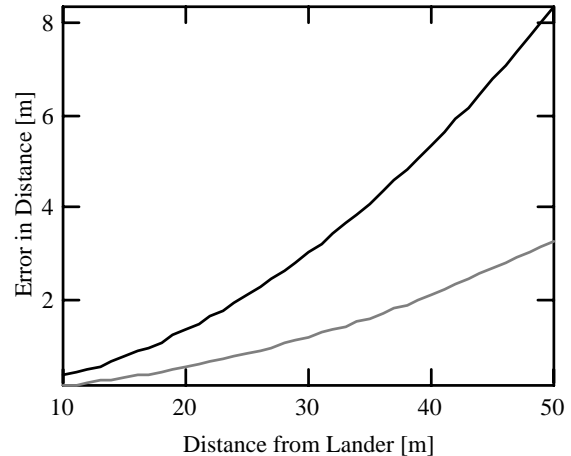


Fig. 5: Errors in distance measurements for IMP owing to systematic errors in the toe-in angle of  $0.5$  mrad (solid line) and random image correlation errors of  $0.2$  pixels (dashed line).

### *The Rover Seen in the IMP Images*

We selected a number of images showing the rover at various distances and orientations with respect to the lander. We identified 4 fiducial marks on the rover; these were essentially the corners of the solar array attached on the top (Fig. 6). The measured positions of these fiducial marks (Table 2) were compared with the known dimensions of the rover, supplied by the rover team (Rover Team, 1997, see Fig. 6). In the example of Fig. 6, the rover was located North of the landing site facing west, at a distance of 3.5 m from the camera. The fiducial mark coordinates indicate that the rover is tilted by  $5.4^\circ$  with respect to the Mars local level. Taking the distances between point 1 and 4 or 2 and 3, the rover was measured to have a length of 41.6 and 42.8 cm, respectively, in excellent agreement with the nominal size of 41.6 cm. This indicates that sizes (e.g. for rocks) can be recovered to better than  $<3\%$ . However, the measurements of the rover's width (taking the distance between point 1 and 2 or 3 and 4) badly suffered from the errors in pixel coordinate measurements, and the unfortunate propagation of errors in this type of geometry with measurements to be taken almost parallel to the line of sight. Note that the errors in distance measurements are much larger than the errors in the measurements of position in the image plane. The width of the rover in the example of Fig. 6 was recovered to within 10% only. The test indicated that apparent sizes of objects can be reliably measured, with their "depths" remaining uncertain to a high degree.

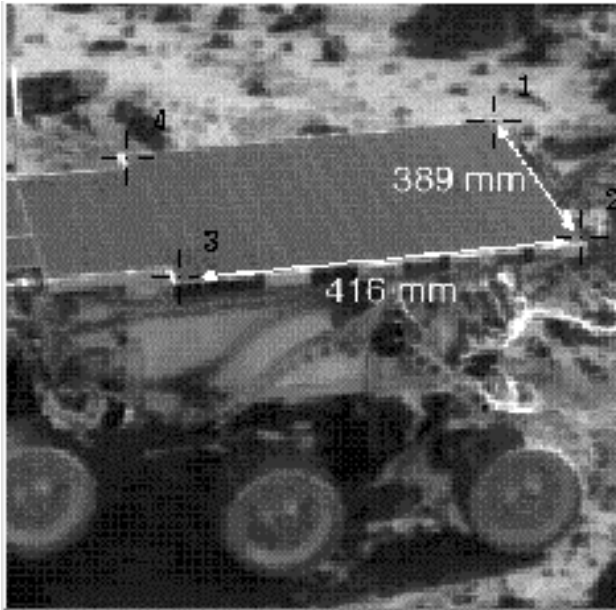


Fig. 6: The rover "Sojourner" and the positions of fiducial marks used to estimate the rover's distance from the lander (note the high data compression of the image).

ID	left ns	left nl	right ns	right nl
1	212.00	56.00	212.62	57.29
2	236.00	87.00	233.67	87.67
3	127.00	98.00	124.33	98.67
4	113.00	65.00	114.00	65.33

ID	X	Y	Z
1	-3.658	-1.1741	-0.0764
2	-3.297	-1.167	-0.0603
3	-3.3141	-0.7418	-0.014
4	-3.7401	-0.77	-0.0156

Table 3: Image (top) and object (bottom) coordinates of fiducial marks on the rover. Object point coordinates were computed adopting a view vector of (0.937, 0.227, 0.266).

## 6 POINTING CALIBRATION

Nominal pointing data with which the camera had been commanded to take a picture was available for each individual image data file. Unfortunately, the stepper motor drive to turn the camera had an angular "play" (backlash) that produced an uncertainty in this pointing information of approximately  $1.5^\circ$  in azimuth and  $0.65^\circ$  in elevation (Britt *et al.*, 1997). Using backlash pointing "rules" this error could be somewhat reduced. Nevertheless, "relative" pointing errors between images became apparent by offsets and gaps in mosaics when compiled using these nominal pointing data. In addition, the "absolute" pointing with respect to the Mars local level (L frame) was known to be uncertain by  $1^\circ$  (see above). An important task was therefore to derive precise absolute pointing data for images. This was needed to produce cartographically accurate panoramas, to compute precise

illumination angles in the terrain for photometric studies, and also to determine precise azimuth angles to horizon features (see companion paper, Oberst *et al.*, 1998).

Three sunrise and one sunset image which show the solar disk together with the horizon were selected as "pilot images" for which precise pointing was determined. Ephemeris data were used to determine azimuth and elevation of the sun at the Pathfinder landing site (Fig. 7) at the times the images were taken. The landing site was assumed to be located at the reported coordinates of  $19.327^\circ\text{N}$  (geodetic latitude) and  $33.523^\circ\text{W}$  (see companion paper, Oberst *et al.*, 1998a; Folkner *et al.*, 1997). This fixed the pointing for these images with an estimated precision of 2 pixels, or  $0.11^\circ$ .

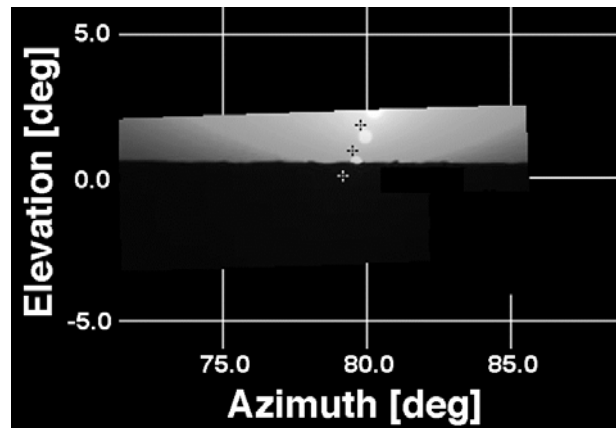


Fig. 7: Composite of three sunrise images used for calibration of camera pointing. The crosses mark the theoretical position of the Sun with respect to azimuth and elevation based on ephemeris data.

## 7 PHOTOGRAMMETRIC PROCESSING

### Reference Horizon Mosaic

We first selected 33 single-filter images from the "Gallery Panorama" (Table 1) that showed the horizon and carried out tiepoint measurements between images. The "Gallery Panorama" was the only one to show the complete horizon with sufficient overlap between images to collect the tiepoints. Block adjustment techniques were used to obtain relative pointing data for this set of images. For one of the images the pointing was assumed to be correct and held fixed. Using these pointing data, images were converted to a cylindrical map projection ("azimuth/elevation space") and mosaicked. The projection was computed using the given quaternion for the conversion from lander coordinate system to Mars-fixed coordinates (see above). The scale was chosen to be 18 pixels per degree in both vertical and horizontal direction, thus retaining the original image resolution as far as possible. The panorama was then shifted in the horizontal (azimuth) and vertical (elevation) direction to agree with the pointing of the sunrise images. Horizon markings seen in both the panorama and the sunrise images were used to find a precise match between the two. The horizon mosaic thus served as a reference for the panorama and the DTM.

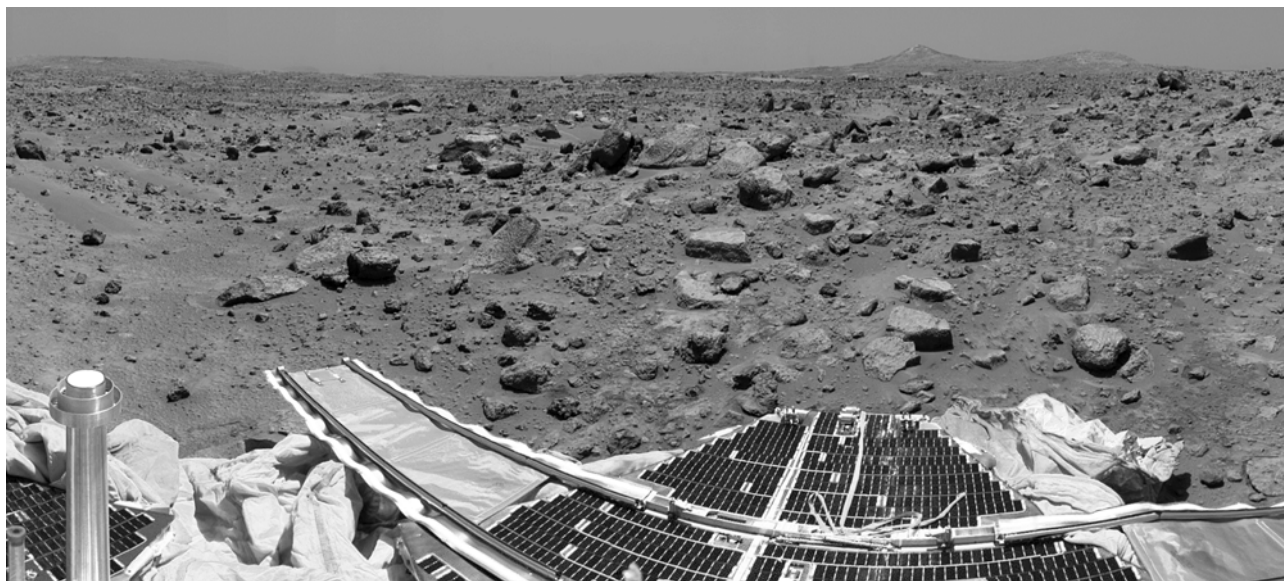


Fig. 8: Section of the monoscopic panorama of the Pathfinder landing site looking southwest.

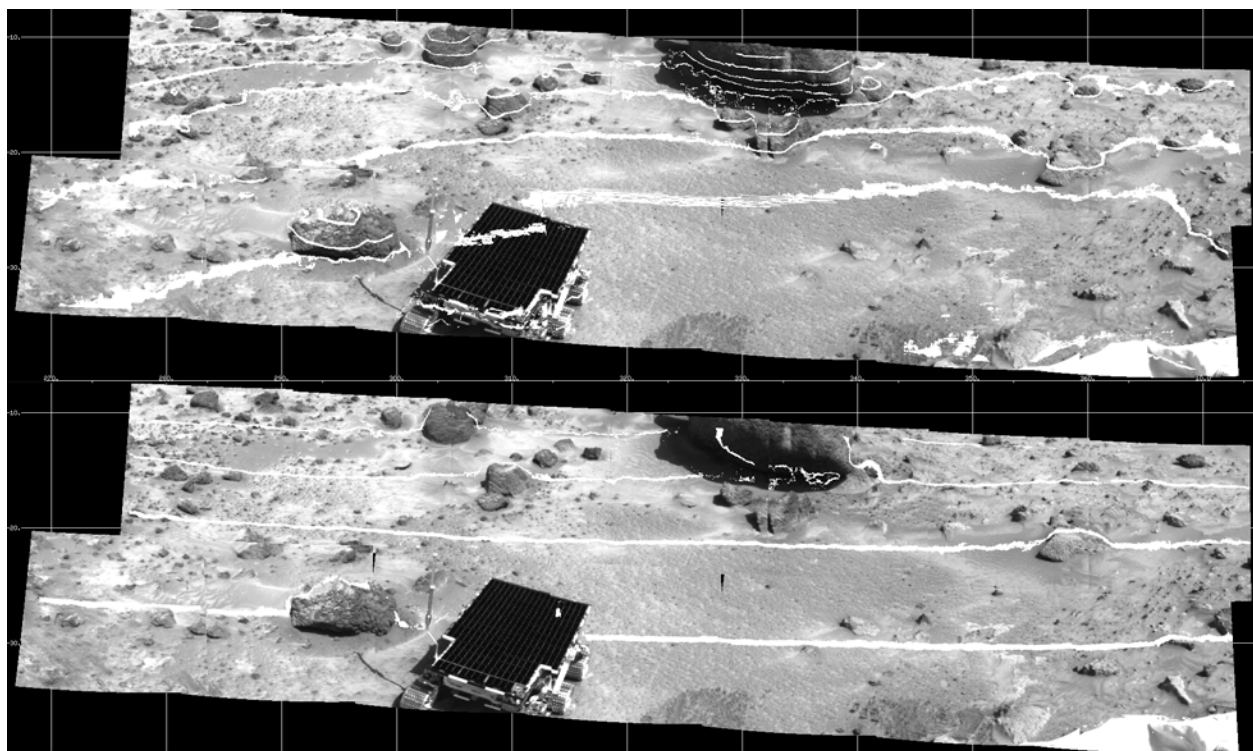


Fig. 9: Part of image panorama with contours of equal-elevation (spacing 10cm; top) and equal-distance (1m; bottom).

*Full Monoscopic Panorama*

A full monoscopic color panorama was compiled on the basis of the "Gallery Pan". It consists of 468 images in the red, green, and blue color filters (156 images in each filter). Beginning with the red filter, all images were

reprojected to azimuth/elevation space and registered one by one to the reference mosaic: Manual tiepoint measurements were used to adjust the nominal pointing of each new image with respect to other images already in place. Images with low elevation angles, for which this



simple approach failed, were geometrically corrected using rubber stretching techniques. The procedure was repeated for images from the green and blue color filters and finally resulted in a seamless semi-controlled color mosaic in a cylindrical projection (Fig. 8) which was used

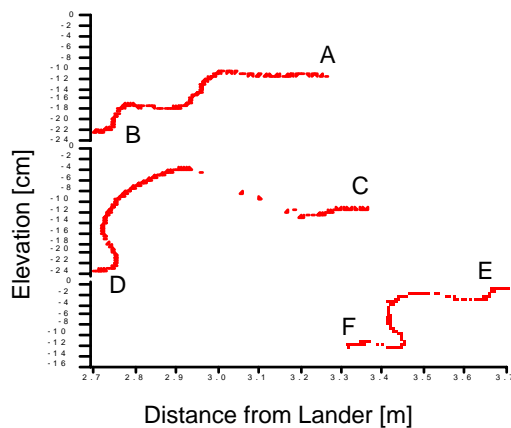
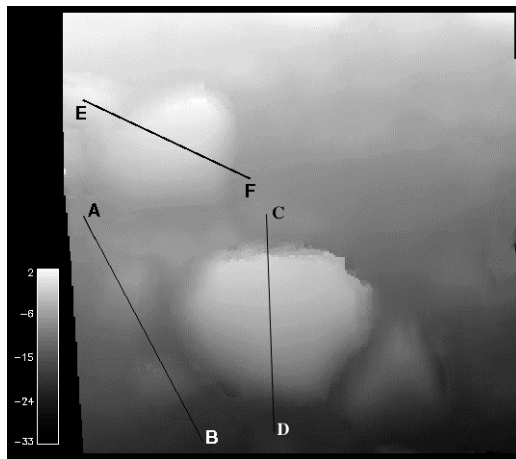
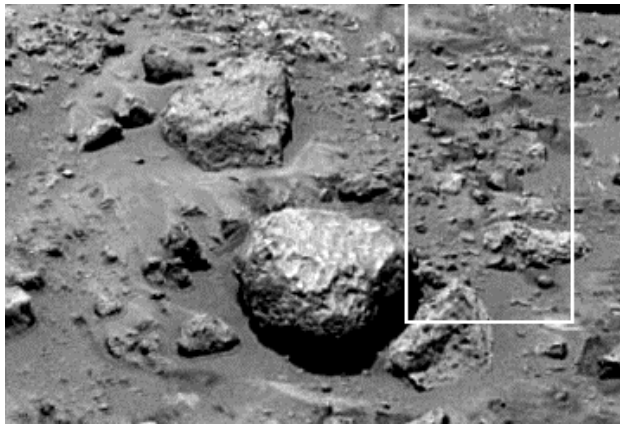


Fig. 10: IMP image showing the rock "Grommit" (top) and a corresponding terrain model of the area in image space to match orientation and scale of the image (middle). Selected elevation profiles are derived from the terrain model (bottom). White box in top view outlines Figure 11. as a basis for geomorphological investigations.

### Terrain Models

The terrain model was based on stereo image data from the "Super Pan" (Table 1); "Monster Pan" images were used where the "Super Pan" suffered from gaps. The software packages described above were used to carry out image matching with the goal to derive large numbers of conjugate points. The resulting line and sample disparities were normally stored in image-formatted files that matched the format of the (left) reference image. Next, object point coordinates were computed from these. Again, files containing the X- Y- and Z-coordinates of the object files were stored in image formatted files. The procedure was carried out for individual image pairs. Interpolation techniques were then used to combine the object point data to large contiguous models. Essentially two types of terrain models were derived, one in the form of a standard topographic map showing the landing site from the top – the other one reprojected to azimuth/elevation space to precisely match the format of the image panorama. Plots of equal-distance and equal-elevation contours were derived and superposed on the panorama (Fig. 9). This format also allows to extract elevation profiles very easily (Fig. 10).

The terrain model yielded good terrain coverage up to a range of approx. 50m and thus was an important basis for mapping of the landing site and. In particular, it was used to derive precise distances and sizes for approx. 2000 rocks seen in the images (Hauber *et al.*, 1998). The model indicates that the lander is located on the flank of a broad, gentle ridge with northeast trend.

### Surface Slopes

The terrain model was heavily used to analyze surface slopes in the lander area. We developed interactive software tools that allowed us to extract precise solar incidence, emission, and phase angles, as well as corresponding pixel DN values from any position in the DTM and the corresponding image panorama, taking advantage of the fact that the DTM and panoramas had been processed in matching projections and scales. This tool gave us the unique opportunity to study variations in the apparent brightness of surface material with solar

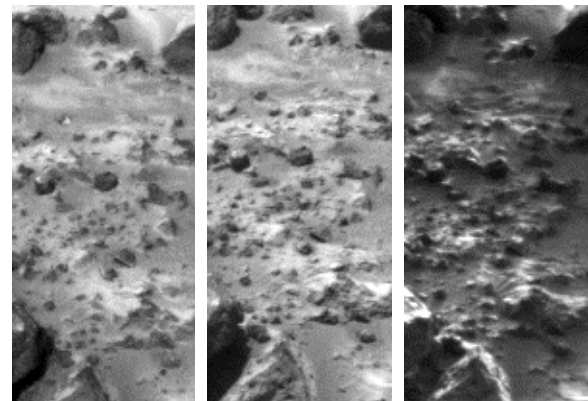


Fig. 11 Mars Pathfinder images taken for photometric studies (see Fig.10 for location) showing the surface under different lighting conditions at different times of the day (left: 08:09, middle: 11:58, right: 17:08). illumination for comparison with analytical photometric functions and laboratory data.

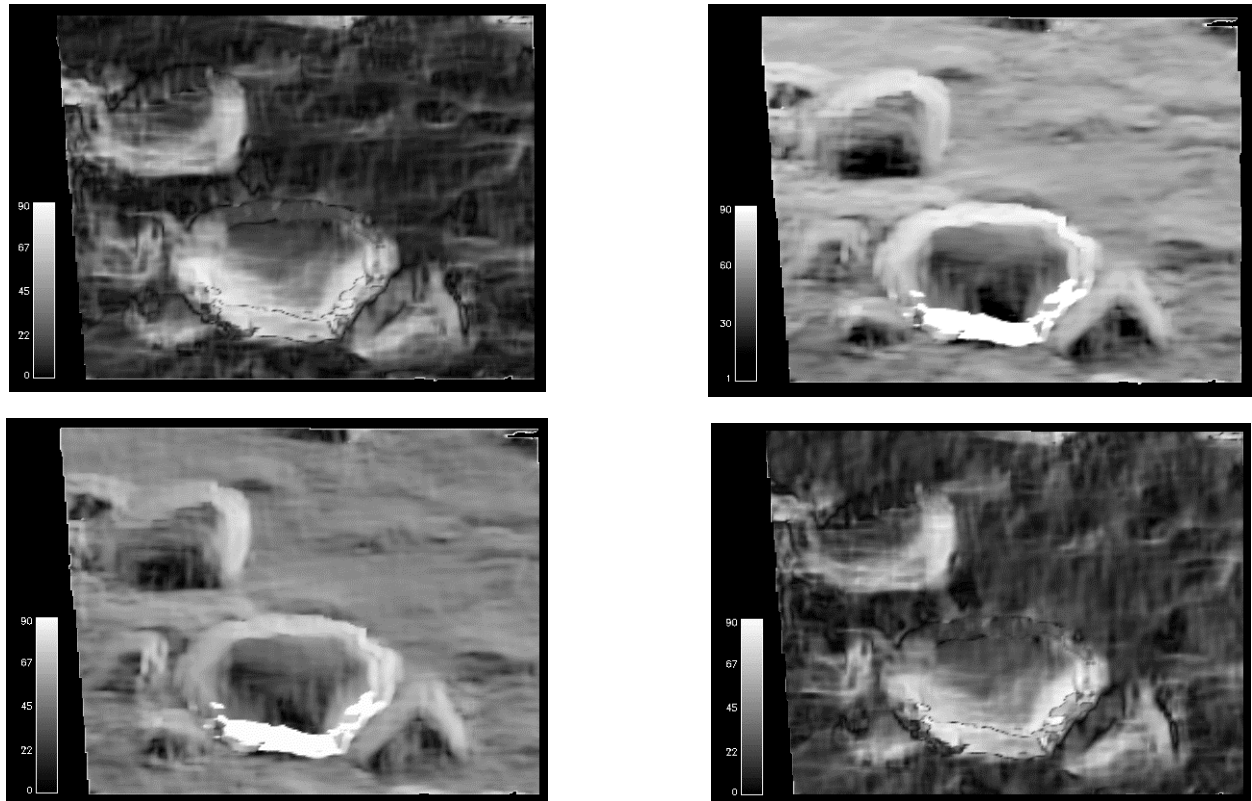


Fig. 12: Thematic image (cf Fig. 10 for raw image) showing the Z component of the surface normal vector (a) and the emission angle (b) (angle between the surface normal and the observer).

## 8 DISCUSSION AND OUTLOOK

The Pathfinder mission was highly successful and has generated overwhelming excitement in the exploration of Mars. From the experience we have gathered during this project, we wish to report on a number of lessons learned, which could help in the design, planning, and operation of future lander missions and imaging experiments. Overall, we suggest that more emphasis should be placed on the precision mapping of the landing site and on the potential of the image data for photogrammetric analysis. Future cameras should be equipped with larger-array CCDs to avoid excessive data processing time and costs. This would also make the block adjustment more stable and improve the geometric accuracy of panoramas and DTMs. Also, the pointing capability of the camera should be improved to avoid the cumbersome reconstruction of the pointing vectors from the image data. We suggest that rovers be equipped with more fiducial marks, e.g. a clearly visible grid pattern, for a quick verification of camera calibration and operation of the software. In addition, we suggest to attach more fiducial marks on the lander and take images of them in the context of the surrounding terrain to establish relationships between the lander and planet-fixed coordinate frames. Also, acquiring more images of the Sun near the horizon would be an important asset to cartographic work. These images could be used to refine estimates of the North direction including errors. In addition, images taken many weeks or months apart would allow us to make an independent check on the

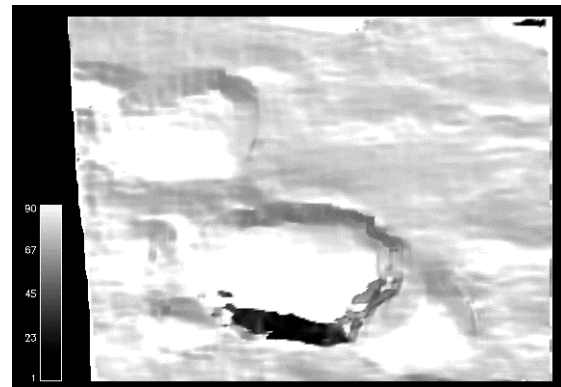


Fig. 13 Thematic image (cf. Fig. 10 for raw image) showing the solar incidence angle (angle between the surface normal and the direction of the sun) as it changes with time of day as in Fig. 12 (a: 08:09, b: 11:58, c:17:08). Note that the solar incidence angles, measured from the surface normal, are lowest around noon. Areas with angles smaller than  $0^\circ$  and larger than  $90^\circ$  are in shadow.

position of the lander on the planet.

Future missions to the "Red Planet" include the Mars Polar Lander to be launched by the end of this year. The lander will have a camera, identical to that carried by Pathfinder; however, a different stepper motor design has been chosen which is expected to improve the predictability of the camera pointing (P. Smith, pers. comm.). In 2001, the Mars Surveyor '01 orbiter and lander mission will be launched. The lander will carry the "Athena" rover, designed to roam the surface of Mars within several tens of kilometers of the landing site within its expected lifetime of about one year. Athena will have a

color stereo camera similar to IMP; the design of this camera is in the planning stage. A similar mission of this US Mars Surveyor program will be launched in 2003. Finally, in this same year, the European Mars Express Mission is scheduled to launch and deploy a set of three or four surface landers. Each of them will carry multispectral stereo cameras that will feature larger-array (1024x1024) CCDs.

Acknowledgements. We wish to thank our colleagues from the Mars Pathfinder science team who designed and successfully operated the lander's imaging experiment. We also wish to thank data system developers at JPL, in particular V. Parizher, J. Lorre and A. Runkle, who provided important software contributions to this study.

## 9 REFERENCES

- Britt, D.T., Maki, J., and Weinberg, J., Users Guide: The Imager for Mars Pathfinder, The University of Arizona (unpublished), Tucson, 1997.
- Folkner, W.M., C.F. Yoder, D.N Yuan, E.M. Standish, and R.A. Preston, Interior structure and seasonal mass redistribution of Mars from radio tracking of Mars Pathfinder, *Science* 278, 1749-1752, 1997.
- Gaddis, L.R., Soderblom, L.A., Kirk, R.L., Johnson, J.R., Ward, A.W., Barrett, J., Becker, K., Becker, T., Blue, J., Cook, D., Eliason, E., Hare, T., Howington-Kraus, E., Isbell, C., Lee, E.M., Redding, B., Sucharski, R., Sucharski, T., Smith, P.H., Britt, D.T., and The Pathfinder Science Team, Digital Mapping of the Mars Pathfinder Landing Site: Design, Acquisition, and Derivation of Cartographic Products for Science Applications, *J. Geophys. Res.*, 1998, in press.
- Golombek, M.P., The Mars Pathfinder Mission, *J. Geophys. Res.*, Vol. 102, No. E2, 3953-3965, 1997.
- Golombek, M.P., Cook, R.A., Economou, T., Folkner, W.M., Haldemann, A.F.C., Kallemeyn, P.H., Knudsen, J.M., Manning, R.M., Moore, H.J., Parker, T.J., Rieder, R., Schofield, J.T., Smith, P.H., and Vaughan, R.M., Overview of the Mars Pathfinder Mission and Assessment of Landing Site Predictions, *Science*; 278, 1743-1748, 1997.
- Hauber, E., Jaumann, R., Mosangini, C., Russ, N., Trauthan, F., Matz, K.-D., and Fabel, O., Rocks at the Pathfinder Landing Site, Mars: Identification and Size Distribution; LPS; XXIX; Lunar and Planetary Institute; Houston (CD-ROM), 1998.
- Kirk, R.L., Howington-Kraus, E., Hare, T., Dorrer, E., Cook, D., Becker, K., Thompson, K., Redding, B., Blue, J., Galuszka, D., Lee, E.M., Gaddis, L.R., Johnson, J.R., Soderblom, L.A., Ward, A.W., Smith, P.H., Britt, D.T., and The Pathfinder Science Team; Digital Photogrammetric Analysis of the IMP Camera Images: Mapping the Mars Pathfinder Landing Site in Three Dimensions, *J. Geophys. Res.*, 1998, in press.
- Mellstrom J., and K. Lau, Mars Pathfinder Aim Phasing and Coordinate Frame Document, JPL, PF-300-4.0-04, 1996.
- Oberst, J., Jaumann, R., Zeitler, W., Hauber, E., Kuschel, M., Parker, T., Golombek, M., Malin, M., and Soderblom, L., Photogrammetric analysis of horizon panoramas: The Pathfinder landing site in Viking Orbiter images, *J. Geophys. Res.*, 1998, in press.
- Oberst, J., Wählisch, M., Zeitler, W., Hauber, E., and Jaumann, R., Mars Pathfinder: Cartographic Analysis of the Landing Site from Orbit, ISPRS, this volume, 1998.
- Rieder, R., Wänke, H, Economou, T., and Turkevich, A.; Determination of the Chemical Composition of Martian Soil and Rocks: The Alpha Proton X Ray Spectrometer; *J. Geophys. Res.*, Vol. 102, No. E2, 4027-4044, 1997.
- Rover Team; The Pathfinder Microover; *J. Geophys. Res.*, Vol. 102, No. E2, 3989-4001, 1997.
- Seiff, A., Tillman, J.E., Murphy, J.R., Schofield, J.T., Crisp, D., Barnes, J.R., LaBaw, C., Mahoney, C., Mihalov, J.D., Wilson, G.R., and Haberle, R.; The Atmosphere Structure and Meteorology Instrument on the Mars Pathfinder Lander, *J. Geophys. Res.*, Vol. 102, No. E2, 4045-4056; 1997.
- Smith, P.H., Tomasko, M.G., Britt, D., Crowe, D.G., Reid, R., Keller, H.U., Thomas, N., Gliem, F., Rueffer, P., Sullivan, R., Greeley, R., Knudsen, J.M., Madsen, M.B., Gunnlaugsson, H.P., Hviid, S.F., Goetz, W., Soderblom, L.A., Gaddis, L., and Kirk, R., The Imager for Mars Pathfinder Experiment, *J. Geophys. Res.*, Vol. 102, No. E2, 4003-4025, 1997a.
- Smith, P.H., Bell III, J.F., Bridges, N.T., Britt, D.T., Gaddis, L., Greeley, R., Keller, H.U., Herkenhoff, K.E., Jaumann, R., Johnson, J.R., Kirk, R.L., Lemmon, M., Maki, J.N., Malin, M.C., Murchie, S.L., Oberst, J., Parker, T.J., Reid, R.J., Sablotny, R., Soderblom, L.A., Stoker, C., Sullivan, R., Thomas, N., Tomasko, M.G., Ward, W., and Wegryn, E., Results from the Mars Pathfinder Camera, *Science* 278, 1758-1765, 1997b.